

## **SUPPLEMENTAL INFORMATION**

### **Essential Role of Presynaptic NMDA Receptors in Activity-Dependent BDNF Secretion and Corticostriatal LTP**

Hyungju Park, Andrei Popescu, Mu-ming Poo

This Supplementary Information includes:

**- Supplemental figures and legends**

Figure S1, related to Figure 1.

Figure S2, related to Figure 2.

Figure S3, related to Figure 3.

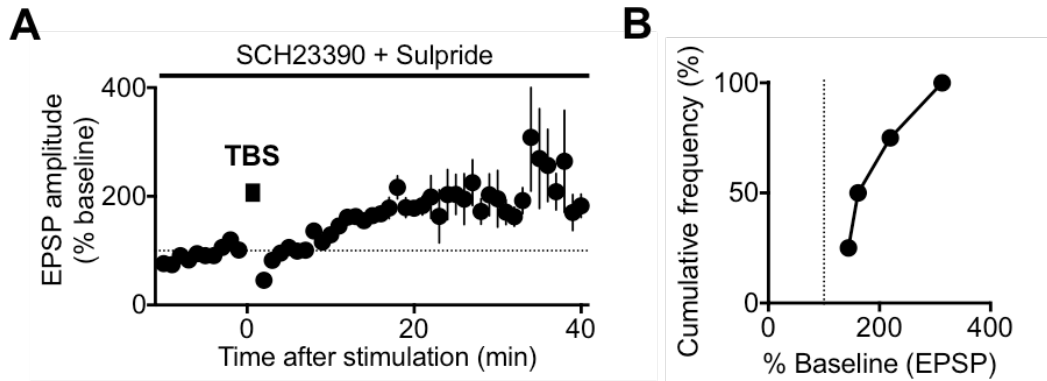
Figure S4, related to Figure 4.

Figure S5, related to Figure 5.

**- Experimental Procedures**

**- References**

## SUPPLEMENTAL FIGURES and LEGENDS

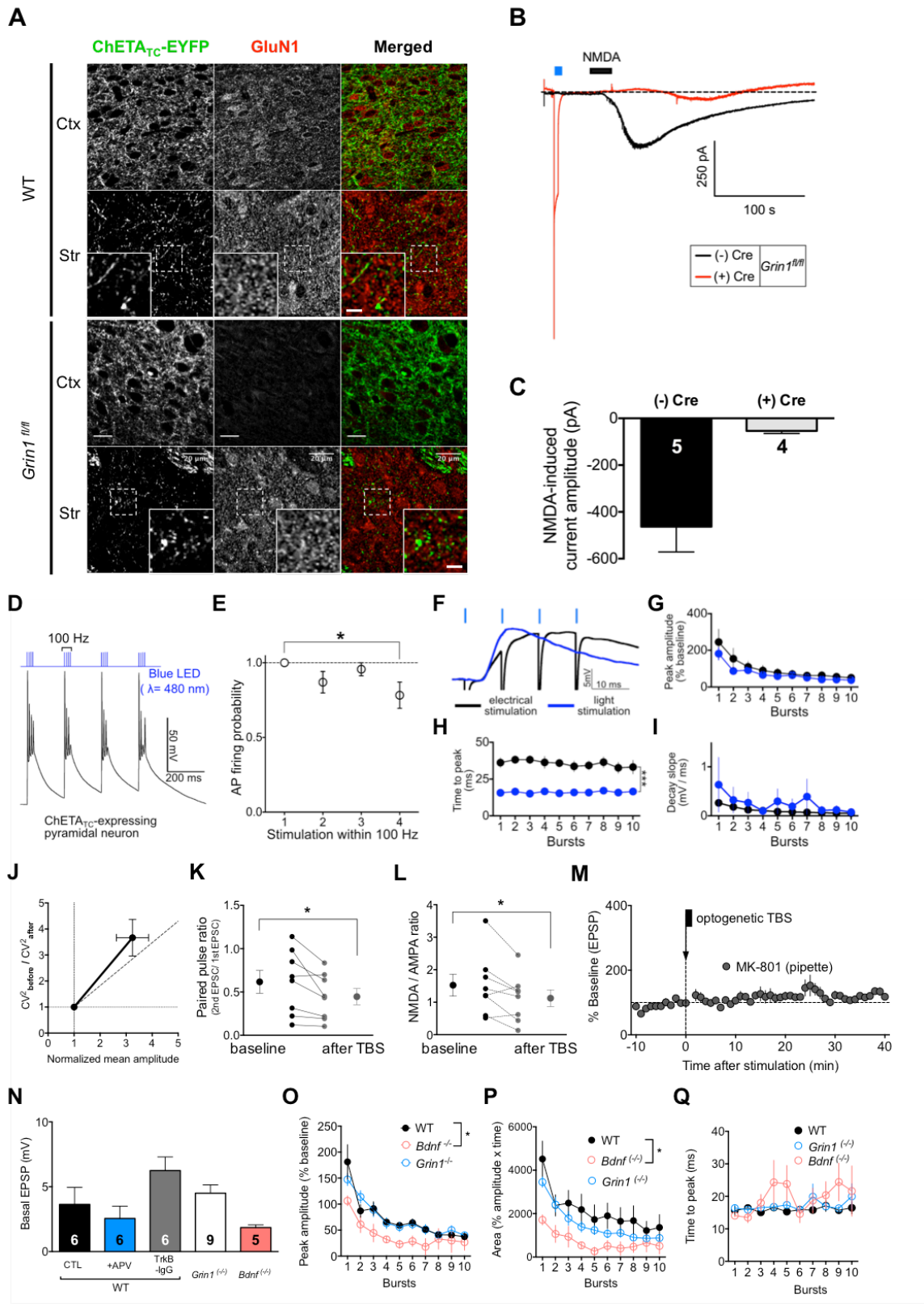


**Figure S1**

**Figure S1 (related to Figure 1). Dopamine signaling is not involved in TBS-induced corticostriatal LTP.**

(A) Summary of LTP induction by electrical stimulation with the TBS pattern in the presence of antagonists for D1/D5 receptor (SCH23390; 10  $\mu$ M) and D2 receptor (sulpride; 10  $\mu$ M). Mean  $\pm$  s.e.m. (n = 4 slices, from 2 mice).

(B) Cumulative percentage plot of mean EPSP amplitudes during 30 - 40 min after TBS. (% of baseline, mean  $\pm$  s.e.m; 210  $\pm$  38 %).



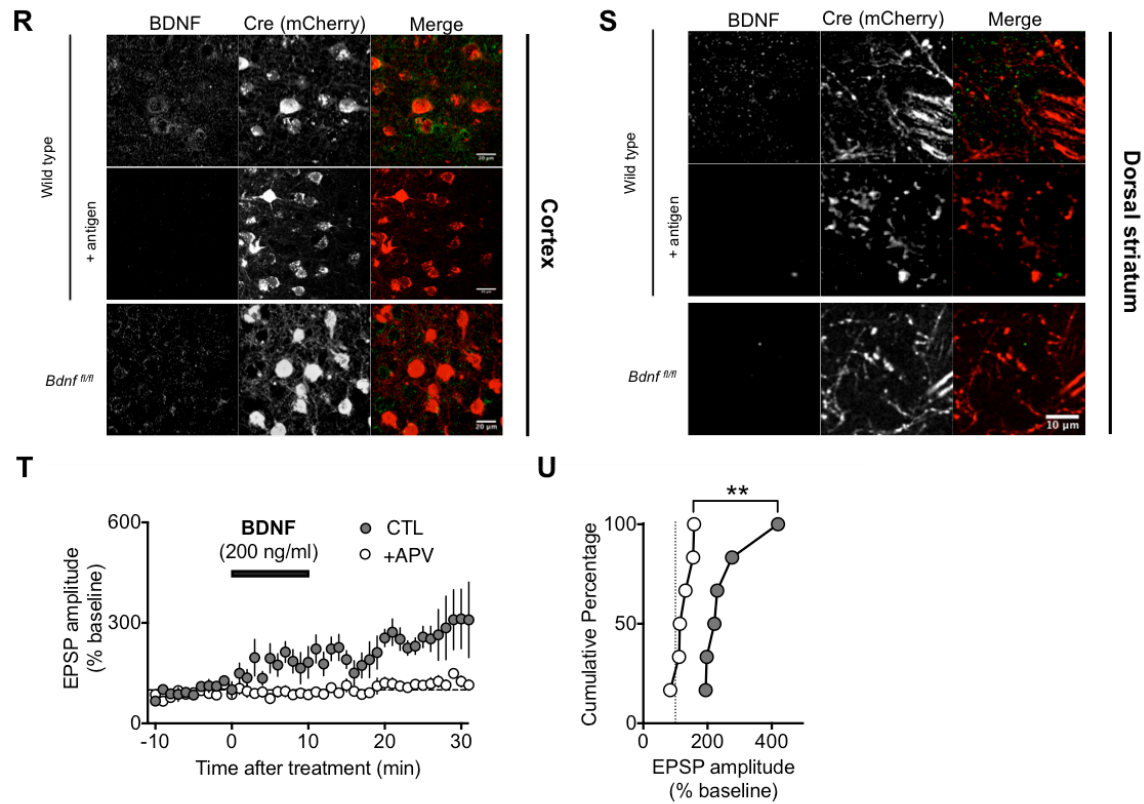


**Figure S2**

**Figure S2 (related to Figure 2). Cre-dependent deletion of GluN1 and BDNF, and further analyses of TBS-LTP**

(A) Immunostaining showing GluN1 expression in M1 neurons (Ctx) and M1-derived axons in the striatum (Str) of wild-type (WT) mice or *Grin1<sup>fl/fl</sup>* mice that were injected with AAV-Cre-2a-mCherry and AAV-DIO-ChETA<sub>TC</sub>-YFP. Normal GluN1 staining was observed in the ChETA<sub>TC</sub>-YFP-expressing M1 neuron (upper panel) or axons derived from the M1 (lower panel) in WT mice, whereas GluN1 staining was absent in ChETA<sub>TC</sub>-YFP-expressing M1 neurons or M1-derived axons in *Grin1<sup>fl/fl</sup>* mice. *Inset*: images of representative cortical axons at a higher resolution (dotted box). Scale bar = 5  $\mu$ m.

(B) Representative recording traces showing whole-cell currents induced by light (blue bar) and NMDA application (black bar) measured from M1 neurons of *Grin1<sup>fl/fl</sup>* mice. Whole-cell inward currents (at the holding potential of -70 mV) in response to bath application of NMDA (50  $\mu$ M) were measured from ChETA<sub>TC</sub>-EYFP-expressing (Cre-expressing; “(+) Cre”) cortical neurons or neighboring cortical neurons with no ChETA<sub>TC</sub>-EYFP (“(-) Cre”). Note that neurons displaying the current induced by a pulse of blue LED light (480nm; 10 s) did not respond to bath application of NMDA, whereas the neurons without the light-induced current showed a large NMDA-induced inward current.

(C) Summary of NMDA-induced currents (mean amplitude  $\pm$  s.e.m.). Numbers of tested cells from three slices of two mice are shown with the bars. (-) Cre,  $-463 \pm 108$  pA; (+) Cre,  $-54 \pm 11$  pA;  $p < 0.05$ , unpaired t-test.

(D) A representative whole-cell recording from ChETA<sub>TC</sub>-expressing cortical pyramidal neurons, showing light-induced depolarization responding to light illumination with a TBS pattern.

(E) Summary of spiking probability (mean  $\pm$  s.e.m.) in response to LED light pulses (4 stimuli at 100 Hz), recorded from ChETA<sub>TC</sub>-expressing M1 neurons ( $n = 4$ ). \*,  $p < 0.05$ ; one-way *ANOVA* with *post-hoc* test.

(F) Representative traces of composite EPSPs evoked by electrical stimulation of cortical axons not expressing ChETA<sub>TC</sub> (black) and by light stimulation of cortical axons expressing ChETA<sub>TC</sub> (blue). Downward spikes superimposed on the electrically evoked EPSP are stimulus artifacts.

(G) Summary of the peak amplitudes of composite EPSPs (% baseline; mean  $\pm$  s.e.m.) induced by TBS-patterned electrical stimulation (black) or light stimulation (blue).

(H) Summary of the time-to-peak of composite EPSPs (mean  $\pm$  s.e.m.) induced by TBS-patterned electrical stimulation or light stimulation. Same color codes as in (G). \*\*\*,  $F(3, 240) = 94.25$ ,  $p < 0.001$ ; two-way ANOVA.

(I) Summary of the decay slope of composite EPSPs (mean  $\pm$  s.e.m.) induced by TBS-patterned electrical stimulation or light stimulation. Same color codes as in (G).

(J) Summary of the relationship between the averaged ratios of the coefficient of variance squared ( $CV^2$ ) with the averaged normalized mean EPSP amplitude (mean  $\pm$  s.e.m.). The ratio of  $CV^2$  was calculated by dividing  $1/CV^2$  during 30 ~ 40 min after optogenetic TBS ( $1/CV^2_{\text{after}}$ ) with that during the baseline period ( $1/CV^2_{\text{before}}$ ). Normalized mean amplitude was calculated by dividing the mean amplitude during 30 ~ 40 min after TBS with that during the baseline period. Since the  $CV^2$  ratio is independent of postsynaptic responses [ $1/CV^2 = EPSP_{\text{mean}}^2 / \text{Var} = np(1 - p)$ , where  $EPSP_{\text{mean}}$  = mean EPSP amplitude;  $\text{Var}$  = variance of the fluctuations in EPSP amplitude;  $n$  = the number of release sites;  $p$  = probability of quantal releases], when the normalized mean amplitude is larger than 1 (LTP) and  $1/CV^2$  ratio is increased (when points are located on or above the diagonal line), this indicates an increase in the probability of evoked quantal release and/or the number of release sites during LTP expression, suggesting presynaptic modifications by TBS.

(K) Summary of changes in paired-pulse ratio (PPR; inter-stimulation interval = 50 ms) of evoked EPSCs by optogenetic TBS application (mean  $\pm$  s.e.m.;  $n = 8$  slices from 3

mice). Averaged PPRs during 30 ~ 40 min after TBS (gray circles) were compared with those during the baseline period (black circles). \*,  $p < 0.05$ , paired t-test.

(L) Summary of changes in the NMDA/AMPA ratio induced by optogenetic TBS application (mean  $\pm$  s.e.m.;  $n = 7$  slices from 3 mice). The ratio of the amplitude of peak NMDAR-dependent EPSPs to that AMPAR-dependent EPSPs before (black circles) and at 30 to 40 min after (gray circles) TBS were averaged and compared for each cell. \*,  $p < 0.05$ , paired t-test.

(M) Summary of optogenetic LTP experiments for testing the involvement of postsynaptic NMDARs in optogenetic TBS-LTP induction. Mean  $\pm$  s.e.m. ( $n = 5$  slices from 2 mice). MK-801 (1 mM) was included in the pipette solution when whole-cell patch clamp was made on to MSNs in the dorsal striatum. The same light pulses with the TBS pattern as Figure 2 were applied to induce LTP. Compared to WT control slices (data from Figure 2), MK-801 infusion prevented induction of TBS-LTP ( $118 \pm 5\%$ . \*\*,  $p < 0.01$ , CTL vs. MK-801 group; Kolmogorov–Smirnov test).

(N) Summary of the peak amplitude of basal EPSP responses (mean  $\pm$  s.e.m.) in normal ACSF (“CTL”) were compared to those in APV- (“APV”) or TrkB-IgG (“TrkB-IgG”) containing ACSF from striatal slices of wild type mice (WT) or those in normal ACSF from striatal slices of *Grin1<sup>fl/fl</sup>* (“*Grin1<sup>-/-</sup>*”) or *Bdnf<sup>fl/fl</sup>* mice (“*Bdnf<sup>-/-</sup>*”) injected with Cre-expressing AAV into M1. Since the level of axonal ChETA<sub>TC</sub> expression and light-induced presynaptic release were variable, all of baseline EPSP responses from Figure 2E (ranging 1 – 10 mV; evoked by LED light illumination with 0.2 ~ 1 ms of duration and 8 mW/mm<sup>2</sup> of light power) were averaged and compared. Numbers of analyzed baseline EPSPs (same with those of Figure 2E) were indicated in the bar. Partially reduced basal

EPSP amplitudes were detected from striatal slices of *Bdnf*<sup>-/-</sup> compared to those of other groups ( $p = 0.057$ , one-way ANOVA test).

(O) Summary on the peak amplitude of composite EPSPs (mean  $\pm$  s.e.m.) induced by each burst of the TBS-patterned light stimulus train. All data in Figure 2 were included. \*,  $F(2, 160) = 20.85$ ,  $p < 0.001$ ; two-way ANOVA.

(P) Summary on the area of composite EPSPs (mean  $\pm$  s.e.m.) induced by each burst of the TBS-patterned light stimulus train. All data in Figure 2 were included. Same color codes as in (E). \*,  $F(2, 170) = 29.81$ ,  $p < 0.001$ ; two-way ANOVA.

(Q) Summary of time to peak of composite EPSP (mean  $\pm$  s.e.m.) induced by each burst of the TBS-patterned light stimulus train. All data in Figure 2 were included. Same colors with (E). No significance was found.

(R) Immunostaining analysis showing endogenous BDNF expression (green) in M1 neurons of WT mice that were injected with AAV-Cre-2a-mCherry (red). The control peptide antigen for anti-BDNF was pre-incubated with the antibody to validate BDNF staining.

(S) Immunostaining analysis showing endogenous BDNF expression in M1-derived axons in the dorsal striatum of *Bdnf*<sup>fl/fl</sup> mice that were injected with AAV-Cre-2a-mCherry. The control peptide antigen for anti-BDNF was pre-treated with the to validate BDNF staining.

(T) Summary of the effect of exogenous BDNF treatment (for 10 min, black bar) on the amplitude of EPSPs recorded in MSNs in brain slices from WT mice. Mean  $\pm$  s.e.m. (CTL,  $n = 6$  slices, from 3 mice; +APV,  $n = 6$  slices from 2 mice). BDNF (200 ng/ml)



was treated for 10 min (black bar) in the absence (grey circles) or presence of NMDAR blocker (white circles; 100  $\mu$ M of APV).

(U) Cumulative percentage plot of the mean EPSP amplitude (% of baseline, mean  $\pm$  s.e.m;  $276 \pm 72$  %) during 20~30 min after BDNF application, same data set and colors as in (T). \*\*,  $p < 0.01$ , Kolmogorov–Smirnov test.

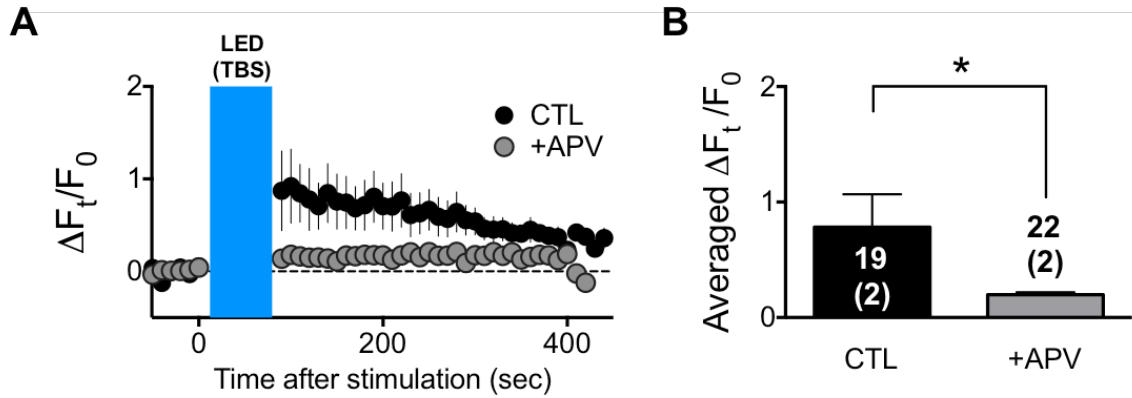


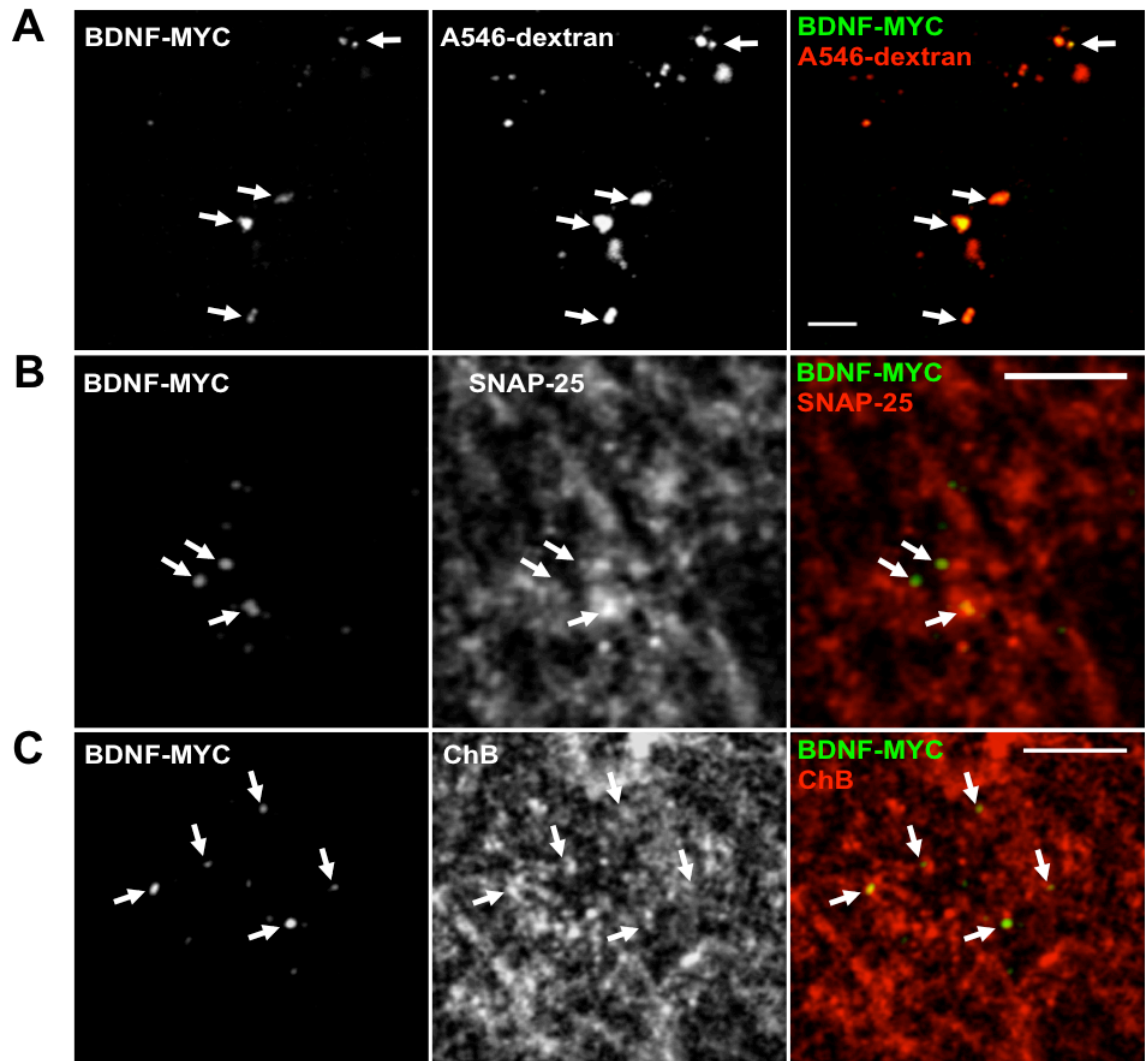
**Figure S3**

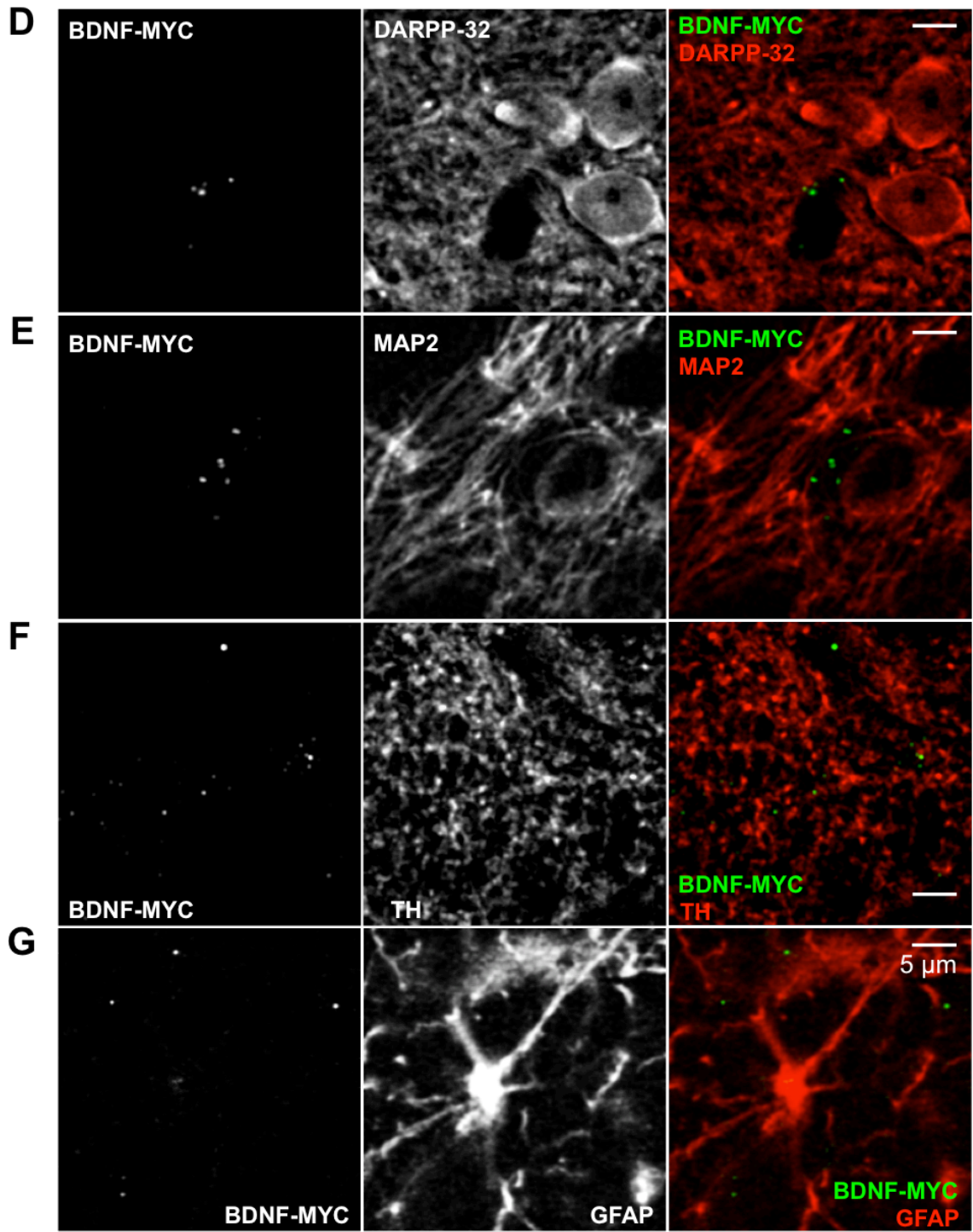
**Figure S3 (related to Figure 3). Prolonged axonal  $\text{Ca}^{2+}$  elevation could be induced by optogenetic stimulation.**

(A) Summary of the average fractional changes of GCaMP5 fluorescence ( $\Delta F_t/F_0$ ) with time at ChETA<sub>TC</sub>-mCherry-expressing axons (mean  $\pm$  s.e.m.) in response to blue light stimulation with the TBS pattern (blue bar), in normal ACSF (CTL) or APV-containing ACSF (+APV).

(B) Summary of average  $\Delta F_t/F_0$  ( $\pm$  s.e.m.) during 100 – 300 s after optogenetic TBS application. Color codes are the same as in (A). Numbers of puncta and slices (with bracket) from two mice are shown with the bars. CTL,  $0.78 \pm 0.29$ ; +APV,  $0.20 \pm 0.02$ .

\*,  $p < 0.05$ , unpaired t-test.





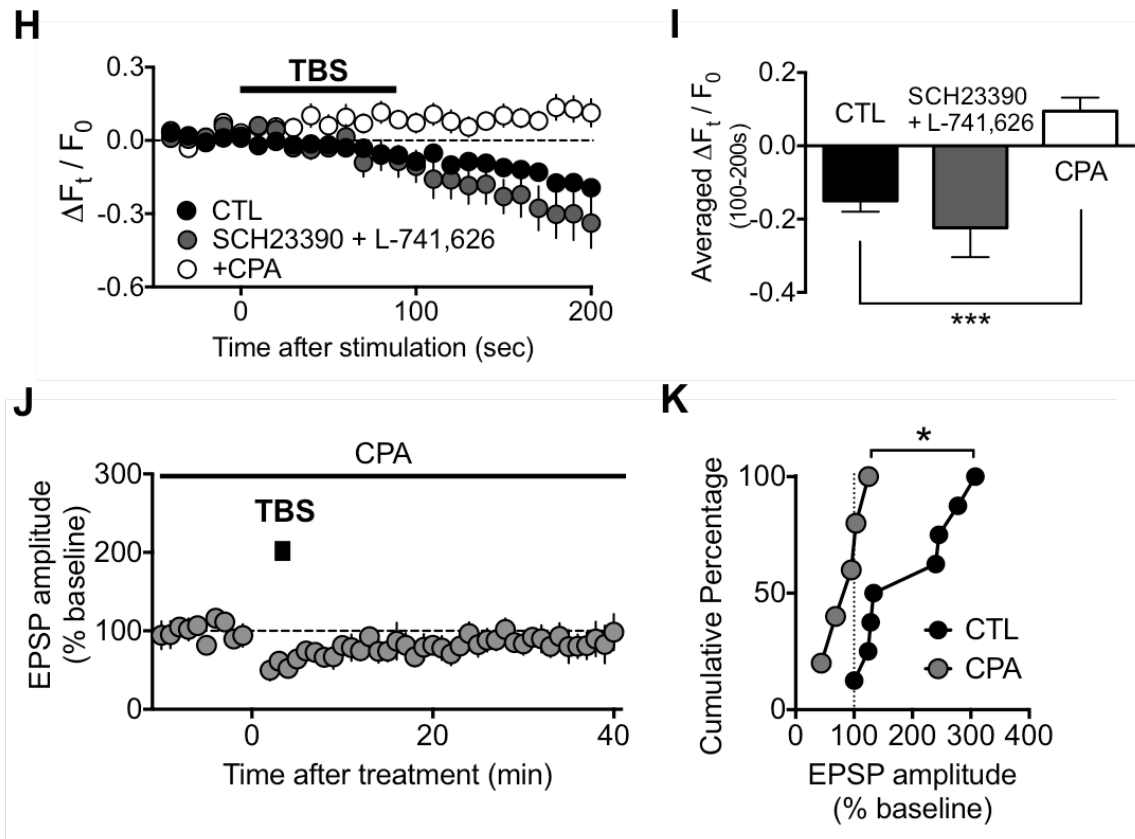


Figure S4

**Figure S4 (related to Figure 4). Localization of endogenous BDNF at secretory granules in cortical axons, and TBS-induced BDNF secretion and LTP are dependent on  $Ca^{2+}$  release from internal stores.**

(A)-(G) Examples of immunostaining images showing co-localization of endogenous BDNF-MYC with Alexa 546-dextran (pre-loaded into M1) (A), with presynaptic marker SNAP-25 (B), and dense-core vesicle marker chromogranin B (C), but not with with the MSN marker DARPP-32 (D), dendritic marker MAP-2 (E), dopaminergic marker TH (F), or glial cell marker GFAP (G).

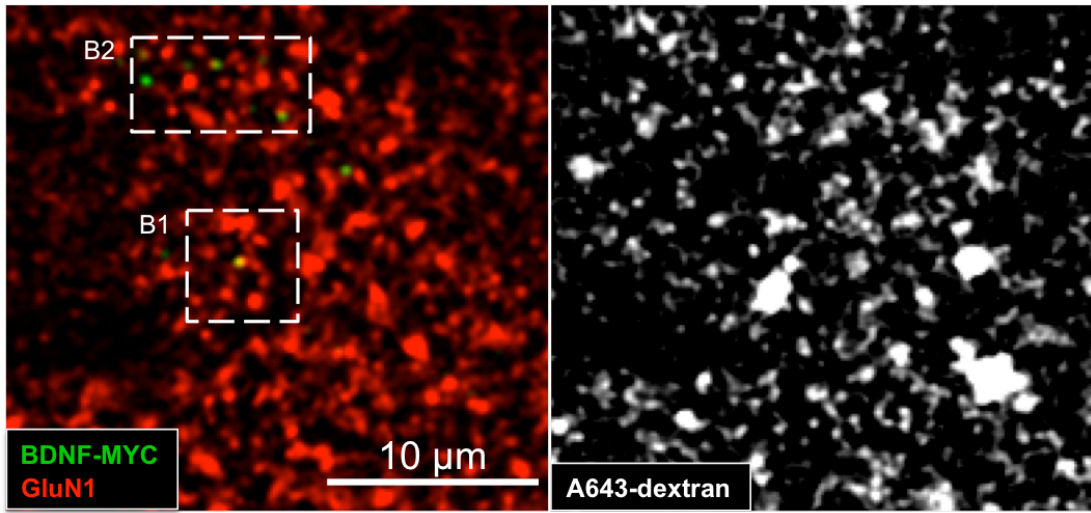
(H) Summary of the average fractional fluorescence changes ( $\Delta F_t/F_0$ ) of axonal BDNF-pHluorin with time in the presence of D1/D5R antagonist (SCH23390; 10  $\mu$ M) and D2R antagonist (L-741,626; 1  $\mu$ M), or inhibitor for  $Ca^{2+}$  release from internal stores (CPA; 30  $\mu$ M). Results of control group (TBS-induced signals in normal ACSF; CTL) were the same as in Figure 4

(I) Bar graphs depict the average  $\Delta F_t/F_0$  ( $\pm$  s.e.m.) during 100 – 200 s after TBS application. Results of control group (TBS-induced signals in normal ACSF; CTL) were the same as in Figure 4. \*\*\*,  $p < 0.001$ , one-way ANOVA with *post-hoc* test.

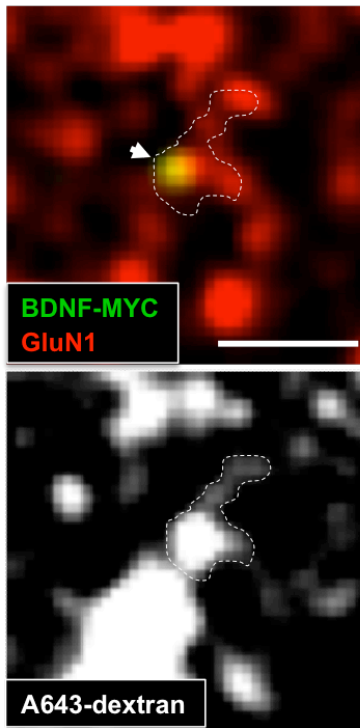
(J) Summary of LTP induction by electrical stimulation with the TBS pattern when intracellular  $Ca^{2+}$  store was depleted by pretreatment with CPA (30  $\mu$ M). Mean  $\pm$  s.e.m. (n = 5 slices, from 2 mice).

(K) Cumulative percentage plot of mean EPSP amplitudes during 30 - 40 min after TBS. Results of control group (TBS-LTP in normal ACSF; CTL) were the same as in Figure 2. % of baseline during 30 ~ 40 min after TBS in CPA group,  $87 \pm 14$  % (mean  $\pm$  s.e.m.). \*,  $p < 0.05$ , Kolmogorov–Smirnov test.

**A**



**B1**



**B2**

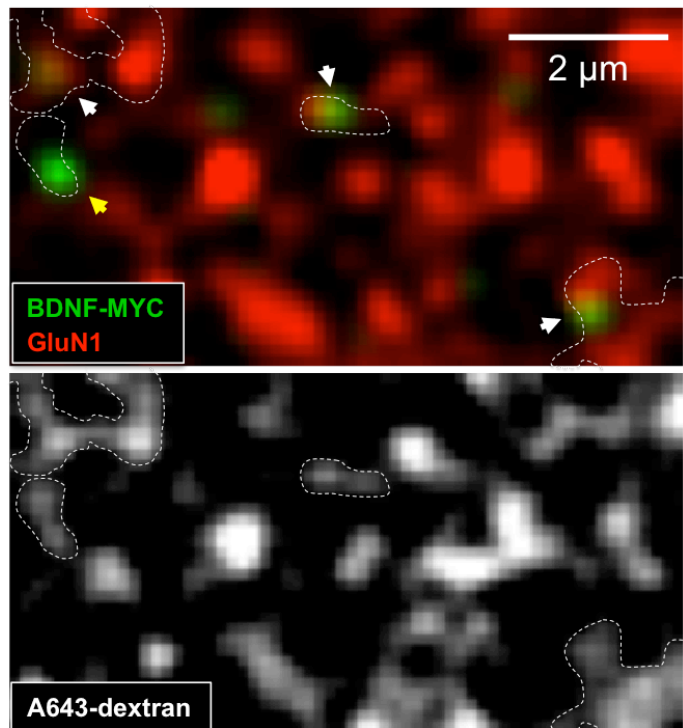


Figure S5

**Figure S5 (related to Figure 5). Endogenous BDNF is localized to M1-derived axons expressing NMDARs.**

(A) *Left*: representative images showing immunostained endogenous BDNF (BDNF-MYC) and NMDARs (GluN1) in the dorsal striatum. *Right*: M1-derived axons were identified by pre-loaded A643-dextran in M1. Dotted boxes: examples of BDNF-MYC signals in M1-derived axons (see below).

(B1) and (B2) Magnified view of dotted boxes in (A). *Above*: examples of colocalization of BDNF-MYC with GluN1 in the dorsal striatum. The borders of M1-derived axons (filled by A643-dextran) were marked by white dotted lines. White arrowheads: BDNF-MYC signals localized to axons labeled with both A643-dextran and GluN1. Yellow arrowhead: BDNF-MYC signals localized to axons filled with A643-dextran but did not contain GluN1. *Below*: same area of B1 showing axons labeled by M1-injected A643-dextran.



## EXPERIMENTAL PROCEDURES

### Reagents

SCH23390, sulpride, L-741,626, NMDA, MK-801, DL-APV, cyclopiazonic acid (CPA), and picrotoxin were purchased from Tocris. TrkB-IgG was purchased from R&D Systems. Other chemicals were purchased from Sigma.

### CV analysis

Coefficient of variance (CV) of light-evoked EPSPs was calculated according to the following equation (Faber and Korn, 1991):

$$CV = [(1-p)/np]^{1/2} = \sigma / M$$

where  $\sigma$  is the standard deviation, and  $M$  is the mean amplitude of synaptic responses. Mean amplitude and standard deviation of EPSPs were obtained from 10 min epochs (20 events) before and 30 min after induction of TBS-LTP. The ratio of  $1/CV^2$  was plotted with the normalized mean amplitude ( $EPSP_{\text{after TBS}}/EPSP_{\text{baseline}}$ ).

### PPR & NMDA/AMPA ratio

To prepare coronal striatal slices (400  $\mu\text{m}$ ) expressing ChETA<sub>TC</sub>-EYFP at cortical axons, *Emx1-Cre* mice injected with AAV-DIO-ChETA<sub>TC</sub>-EYFP were deeply anesthetized with isoflurane, and then transcardially perfused with ~20 ml of slicing ACSF (ACSF containing 10 mM  $\text{Mg}^{2+}$  and 0.5 mM  $\text{Ca}^{2+}$ ) before the brain was dissected.

Brain slices were prepared using a vibratome (Leica) using ice-cold slicing ACSF (below 4°C) and maintained at 30 - 32°C in normal ACSF for 1 hour before electrophysiological recording or two-photon imaging. Whole-cell EPSCs from MSN cells were recorded at holding potential of -70 mV with the pipette solution contains (in mM) 130 CsMeSO<sub>4</sub>, 7 CsCl, 1 EGTA, 5 QX314, 4 MgATP, 0.3 Na<sub>2</sub>GTP, 10 Na<sub>2</sub>-phosphocreatine and 10 HEPES (pH 7.3, 290-300 mOsm). 0.2~1 ms durations of LED light was illuminated to evoke EPSCs from MSNs. After acquiring stable EPSC responses at least for 10 min, PPRs with 50 ms of ISI were measured. TBS was applied in the current clamp mode. Mean peak amplitudes of 1<sup>st</sup> and 2<sup>nd</sup> EPSCs were obtained from 5 min epochs (10 events) before and 30 min after induction of TBS-LTP. PPRs were generated by dividing peak amplitude of 2<sup>nd</sup> EPSC with that of 1<sup>st</sup> EPSC.

For recording NMDAR-dependent EPSCs, MSNs were slowly depolarized to +40 mV, then light illumination was delivered to evoke NMDAR-dependent EPSCs. 100 μM of DL-APV was treated to test whether the light-evoked EPSCs were dependent on NMDAR activation. AMPAR-dependent EPSCs were acquired by recording the light-evoked EPSCs when MSNs were held at -70 mV. TBS was applied in the current clamp mode. Mean amplitude of light-evoked NMDAR- or AMPAR EPSCs was obtained from 5 min epochs (10 events) before and 30 min after induction of TBS-LTP.

### **BDNF-induced EPSP potentiation**

For measuring BDNF-induced potentiation of EPSPs, recombinant human BDNF (Peptrotech) was dissolved into recording solution [ACSF containing 100 μM picrotoxin and 0.1 % bovine serum albumin (BSA)]. Bath solution (ACSF containing 100 μM

microtoxin) was perfused with the speed of 2 ~ 3 ml / min. Test stimuli with a bipolar electrical stimulator were applied at 0.5 Hz to examine EPSP. After 10 min of stable baseline responses, BDNF (200 ng/ml) was applied in bath with the same bath perfusion rate for 10 min to observe the effect of BDNF on corticostriatal EPSP responses.

### **Optogenetic GCaMP5 imaging**

For optogenetic GCaMP5 imaging (Figure S3), AAV-Flex-GCaMP5 and AAV-EF1a-DIO-ChETA<sub>TC</sub> [hChR2(E123T/T159C)]-mCherry (UNC Vector Core) were co-injected with 1:1 GC ratio (0.5 µl in each hemisphere at a titer of ~1 x 10<sup>12</sup> GC per µl) into M1 of *Emx1-Cre* (6 weeks old). At least 2 weeks were allowed to achieve full expression of GCaMP5 and ChETA-mCherry at cortical axons in the dorsal striatum.

### **Labeling cortical axons with fluorescent tracing dyes**

Fifty nl of Alexa 546- or Alexa 647-labelled dextran (10,000 MW; Invitrogen; 0.1 µg/ml in PBS buffer) were injected into M1 of *Bdnf-myc* knock-in mice (8-10 weeks-old). 3 weeks after injection, mouse brain was isolated for immunohistochemical analysis.

### **Immunohistochemistry**

The mice were deeply anaesthetized with isoflurane and immediately perfused with 0.9 % saline followed by fixation with 2.5 % paraformaldehyde (w/v), 0.1% glutaldehyde, and 15% picric acid in 0.1 M phosphate buffer (PB; pH= 7.4). The brain was removed and post-fixed in the same fixative for 15 hr at 4°C. Post-fixed brain was washed with

0.1M PB and sectioned into 40  $\mu$ m of coronal slices using a vibratome (Leica). Free-floating slices were washed with TBS buffer three times and incubated with blocking solution (5% normal goat or donkey serum, 0.3% Triton X-100 in 1x TBS) for 2 hr at room temperature. For BDNF-MYC staining, 20% normal donkey serum, 0.3 % Triton X-100 in 1 x TBS was used as a blocking agent. Primary antibodies were diluted in blocking solution and treated overnight at 4°C. For BDNF-MYC staining, antibody-treatment solution contained bovine serum albumin (BSA, 3%), normal donkey serum (2%), and Triton X-100 (0.3%). After washing slices with TBS buffer three times, and incubated with diluted secondary antibodies for 2 hour at room temperature. Slices were washed with TBS buffer three times and mounted. Confocal microscope (LSM 510, Zeiss) was used for obtaining fluorescence images. Primary antibodies used: mouse monoclonal anti-synaptophysin IgM (Millipore; 1:200), mouse monoclonal anti-PSD95 IgG (Millipore; 1:200), goat anti-MYC IgG (Santa Cruze; 1:400), rabbit polyclonal anti-GluN1 IgG (abcam; 1:200), rabbit polyclonal anti-MAP2 IgG (Millipore, 1:500), rabbit polyclonal anti-TH IgG (abcam; 1:500), rabbit polyclonal anti-GFAP IgG (Dako; 1:1000), rabbit polyclonal anti-Chromogranin B (abcam; 1:200), rabbit polyclonal anti-SNAP25 (abcam; 1:200), and rabbit polyclonal anti-BDNF (Alomone lab; 1:100). Secondary antibodies used: Alexa 546 goat anti-mouse IgM (1:300) Alexa 555 donkey anti-mouse IgG (1:300), Alexa 488 donkey anti-Goat IgG (1:400), Alexa 647 goat anti-rabbit IgG (1:500). To pre-absorb the anti-BDNF with the control peptide antigen (Alomone lab), same amount of the control antigen was incubated with that of anti-BDNF in the antibody treatment solution before applying to slices.

## **Analysis of image data**

Image processing and analysis were performed by using Image J software (NIH). To analyze the co-localization percentage in Fig. 4C, we counted the number of BDNF-pHluorin puncta co-localizing with presynaptic or postsynaptic markers in the observed area. This BDNF-pHluorin puncta number was then divided with the total number of BDNF-pHluorin puncta in the observed area and expressed as percentage.

To analyze acquired image sequences from two-photon microscopy, image sequences from each condition were equally processed to minimize background signals and images displaying slight X-Y movement were re-aligned by using “StackReg” plugins of Image J software (NIH). Data that showed a continuous drift in fluorescence intensity prior to stimulation were discarded. Changes in fluorescence intensity along each time point were measured using the same software, and then relative change in fluorescence intensity ( $\Delta F_t / F_0$ ) was calculated by a following equation:  $\Delta F_t / F_0 = [F_t - F_0] / F_0$ , where  $F_t$  is fluorescence intensity at the specific time  $t$  and  $F_0$  is the averaged fluorescence intensity prior to stimulation.

## **References**

Faber, D.S., and Korn, H. (1991). Applicability of the coefficient of variation method for analyzing synaptic plasticity. *Biophys J* 60, 1288-1294.